A study of the oxidation kinetics of $CuFeO_2$ in the Cu–Fe–O system

G. C. JAIN, B. K. DAS, RAM AVTAR*
Division of Materials, National Physical Laboratory, New Delhi-110012, India

The oxidation kinetics of $CuFeO_2$ in the Cu–Fe–O system have been studied between 500 and 900° C in an atmosphere containing 1 vol % oxygen in a nitrogen stream using thermogravimetric analysis (TGA). It was found that addition of Fe_2O_3 to the $CuFeO_2$ caused a decrease in the oxidation rate while addition of CuO caused an increase. On increasing the concentration of Fe_2O_3 the activation energy was found to increase from $\sim$ 18 kcal mol^{-1} to $\sim$ 45 kcal mol^{-1} and the exponent 'n' in Avrami's equation $f = 1 - \exp(-kt^n)$ was also observed to increase, from 1.3 to 2.3. On adding CuO to the $CuFeO_2$ in the Cu–Fe–O system the activation energy decreased from $\sim$ 18 kcal mol^{-1} to $\sim$ 8 kcal mol^{-1}. The variation in both values indicates changes in the oxidation mechanisms. The microstructural changes associated with oxidation have been studied using optical microscopy. A model has been proposed to explain the results.

1. Introduction

Copper ferrite is a compound of two transition metal oxides. The valency states of the metallic ions depend on various factors such as the ratio of the metallic ion concentrations, the temperature and the surrounding atmosphere [1]. Therefore, several possible phases, e.g. $CuFe_2O_4$, $CuFeO_2$ and $CuFe_5O_8$ exist in the Cu–Fe–O system [2–5]. In an earlier paper, the authors [1] studied the oxidation of $CuFeO_2$ to $CuFe_2O_4$ and simultaneous precipitation of CuO. The oxidation rate was reported to be maximum at a temperature of 700° C. Both, above and below this temperature, the oxidation rate decreased and depended entirely on the ionic mobility and partial pressure of the oxygen in the surrounding atmosphere.
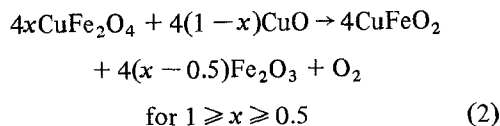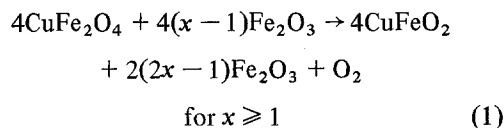
The present work deals with the oxidation of $CuFeO_2$ to $CuFe_2O_4$ when Cu_2O or Fe_2O_3 is present as a second phase. The resulting microstructural changes have also been studied.

2. Experimental procedure
2.1. Material preparation
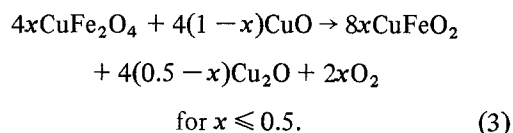In order to prepare material with various compositions, reagent grades of copper oxide and ferric oxide in different molar ratios were mixed in a jar ball mill (shown in Table I). The resultant mixtures were prefired at 800° C for 10 h in air and ball milled again to obtain submicron size powders of homogenous composition. X-ray examination of prefired powders revealed the present of $CuFe_2O_4$ and CuO or Fe_2O_3 phases, depending on whether 'x' is less than or more than 1 respectively. To obtain a polycrystalline powder of $CuFeO_2$, the prefired powders were heated in an inert atmosphere at 900° C in a thermobalance [6]. The weight loss in each sample agreed well with calculated weight loss for one or other of the following reduction reactions.

$$4CuFe_2O_4 + 4(x-1)Fe_2O_3 \rightarrow 4CuFeO_2$$
$$+ 2(2x-1)Fe_2O_3 + O_2$$
$$\text{for } x \geqslant 1 \quad (1)$$

$$4xCuFe_2O_4 + 4(1-x)CuO \rightarrow 4CuFeO_2$$
$$+ 4(x-0.5)Fe_2O_3 + O_2$$
$$\text{for } 1 \geqslant x \geqslant 0.5 \quad (2)$$

---

*Present address: R and D C for Iron and Steel, Steel Authority of India Limited, Ranchi-834002, Bihar, India.

TABLE I Chemical composition of the samples

Sample number	x (mol)	Nominal composition of the oxidation	General formula
1	0.33	$CuO:0.33Fe_2O_3$	—
2	0.50	$CuO:0.5\ Fe_2O_3$	—
3	1.00	$CuO:1.0\ Fe_2O_3$	$(CuO(Fe_2O_3)_x)$
4	1.5	$CuO:1.5\ Fe_2O_3$	—
5	2.0	$CuO:2.0\ Fe_2O_3$	—
6	2.5	$CuO:2.5\ Fe_2O_3$	—

$$4xCuFe_2O_4 + 4(1-x)CuO \rightarrow 8xCuFeO_2$$
$$+ 4(0.5-x)Cu_2O + 2xO_2$$
$$\text{for } x \leqslant 0.5. \qquad (3)$$

Thus $CuFeO_2$ with Cu_2O or Fe_2O_3 was obtained as a second phase. These were further checked by X-ray analysis of the quenched samples held at $900°C$ in a nitrogen atmosphere.

2.2. Thermogravimetric analysis

In order to study the kinetics of the oxidation of $CuFeO_2$ in the presence of Cu_2O or Fe_2O_3, the samples were cooled from $900°C$ down to various temperatures in a nitrogen atmosphere. Such a cooling under nitrogen caused no increase in the weight of the sample, indicating that the samples were not oxidized on cooling to the temperature of interest. 1 vol% oxygen was added to the nitrogen stream and the gain in weight of the sample was monitored isothermally until the weight remained constant. The oxidized samples were analysed by X-ray analysis (Table II) and the presence of $CuFe_2O_4$ $CuFeO_2$, CuO or Fe_2O_3 was detected.

2.3. Metallography

The results of thermogravimetric and X-ray analysis were further confirmed by using optical microscopy. For this purpose, discs of the prefired and milled powders were pressed at a pressure of 1.2 tonne cm^{-2}. The discs were sintered at $900°C$

in a nitrogen atmosphere to obtain a $CuFeO_2$ phase and then quenched to examine the phases present. The surface of the discs was ground about 0.5 mm and polished well by the method given elsewhere [1]. The polished samples were etched in a solution of 50 vol% $HCl + 0.5$ mol% $FeCl_3$. To study the mechanism of oxidation of $CuFeO_2$ to $CuFe_2O_4$ and simultaneous dissolution of Fe_2O_3, the samples were heated in an oxygen atmosphere at $900°C$ for 1 min to 24 h and then quenched. Quenched samples were lapped, polished and thermally etched.

3. Experimental results

The isothermal weight changes in the reduced samples in an atmosphere containing nitrogen with 1 vol% oxygen are shown in Fig. 1 a to d. These curves are plotted for the mass of $CuFeO_2$ oxidized (ΔW) versus time (t) between the temperatures 500 and $700°C$. All the curves show an incubation period which varies with temperature and composition.

The curves in Fig. 1a shows that the oxidation followed a rectilinear law ($\Delta W \alpha t$). The oxidation of $CuFeO_2$ is of a nucleation and growth type process as described earlier [1]. In fact, this composition has two phases: $CuFeO_2$ and Cu_2O, where oxidation of Cu_2O to CuO in 1 vol% oxygen obeys the rectilinear oxidation law [7]. Oxidation of both the phases takes place simultaneously and this is a case of mixed oxidation.

Curves for ΔW against time were plotted for

TABLE II X-ray analysis of phases present

x (mol)	Prefired samples composition	Sample composition in a nitrogen atmosphere at $900°C$	Sample composition in an oxygen atmosphere at 500 to $700°C$
0.33	$CuFe_2O_4 + CuO$	$CuFeO_2 + Cu_2O$	—
0.5	—	$CuFeO_2$	$CuFe_2O_4 + CuO$
1.0	$CuFe_2O_4$	$CuFeO_2 + Fe_2O_3$	—
1.5	$CuFe_2O_4 + Fe_2O_3$	$CuFe_2O_4 + Fe_2O_3$	—
2.0	—	—	—
2.5	$CuFe_2O_4 + Fe_2O_4$	—	—

all compositions, which were oxidized at 600° C. These are shown in Fig. 2. These curves show that for an equal time, a different amount of $CuFeO_2$ oxidized on decreasing the value of x. Hence, it may be concluded that the oxidation rate decreased on increasing the concentration of Fe_2O_3 in the composition.

Similar to the previous work [1], these oxidation data were also found to fit best to Avrami's equation [8]

$$f = 1 - \exp(-kt^n) \qquad (4)$$

where f is $\Delta W/W$, the mass fraction oxidized, t is time, k is oxidation rate constant and n is the exponent.

Fig. 3 shows $\ln\ln(1/(1-f))$ against $\ln(t)$ plots of Equation 4 for composition 4 of Table I. Other compositions in Table I gave similar types of plots. The slope and intercept of these plots give the value of the exponent n and the rate constant k respectively. Exponent n was found to vary from 1.3 to 2.3 as shown in Fig. 4 and the rate constant, k, from 3×10^{-5} to $1 \times 10^{-10} \sec^{-1}$

(Table III) as x varied from 0.3 to 2.5. The variation in the value of exponent n denotes that the oxidation of $CuFeO_2$ to $CuFe_2O_4$ in the presence of Fe_2O_3 changes from a one dimensional oxidation process to a two dimensional oxidation process [9]. These results indicate that the variation in the oxidation rate constant, k, for the oxidation of $CuFeO_2$ to $CuFe_2O_4$ apart from being dependent on the temperature and surrounding atmosphere also depends upon the Fe/Cu ratio.

The activation energy for the oxidation of $CuFeO_2$ to $CuFe_2O_4$ in the presence of Cu_2O and Fe_2O_3 in the Cu–Fe–O system has been calculated from the Arrhenius plots of the rate constants. The value of the activation energy has been found to be nearly equal for the samples for which x varies from 0.5 to 1.0.

The microstructure of the samples in Table I which were sintered at 900° C for 36 h in a nitrogen atmosphere are shown in Fig. 5 a to f. Fig. 5b shows a single phase of $CuFeO_2$ (which is a stable phase below 1005° C [10]) as detected by X-ray diffraction (XRD) analysis. XRD results of the

(c)

(d)
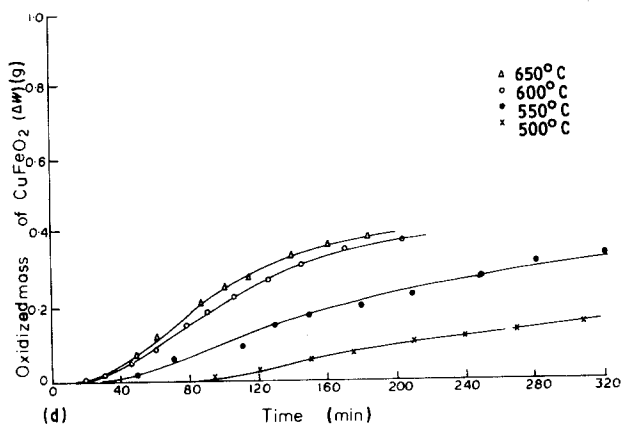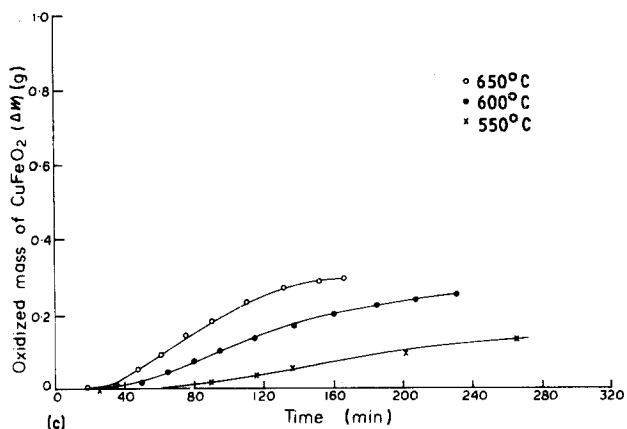
samples also agreed well with the microstructures which are shown in Fig. 5 c to f. These microstructures show the presence of two phases. The concentration of the white phase was seen to vary as x varied from 1 to 2.5. Thus, from the microstructures of Figs. 5 c to f it can be concluded

that the grey and white phases are $CuFeO_2$ and Fe_2O_3 respectively.

The black areas in the micrographs of Figs. 5 c to f are the pores, most of which lie near Fe_2O_3. The concentration of pores seems to increase as the concentration of Fe_2O_3 increases. This may be
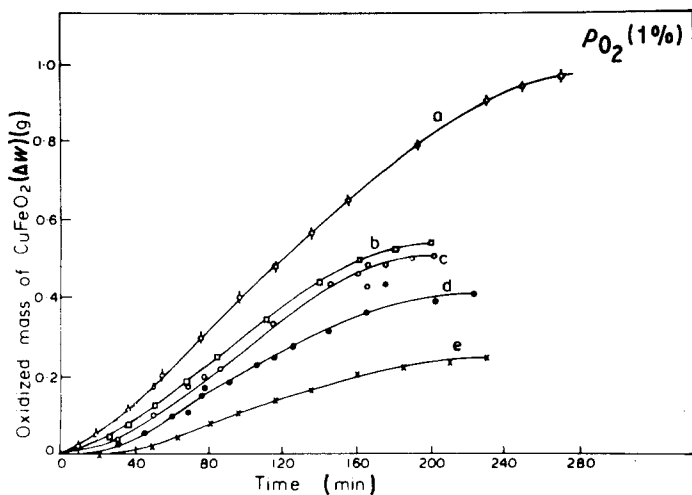
Figure 2 Oxidation of $CeFeO_2$ as a function of time and composition $[CuO(Fe_2O_3)_x]$ at $600°C$ (a) $x = 0.5$ (b) $x = 1.0$ (c) $x = 1.5$ (d) $x = 2.0$ and (e) $x = 2.5$.

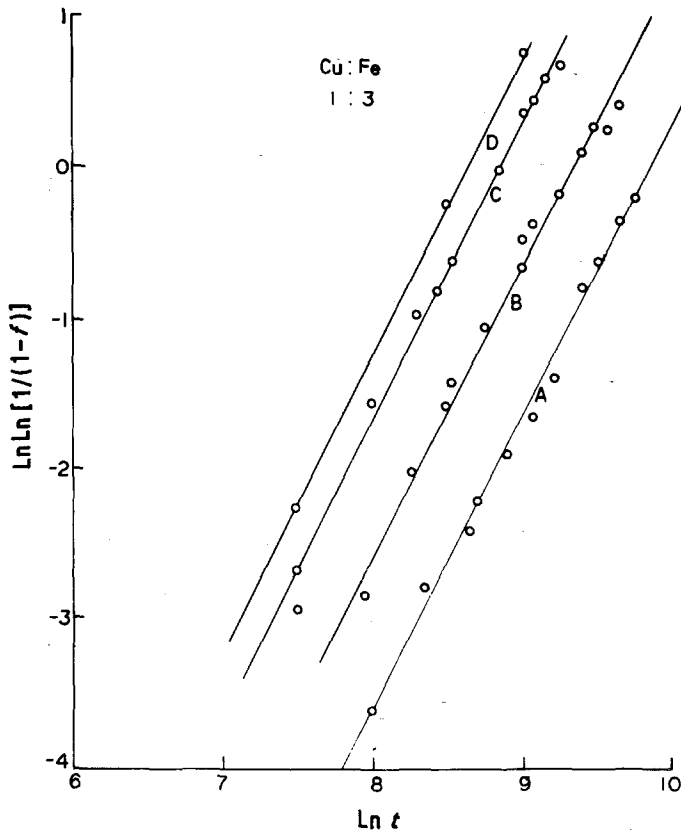*Figure 3* Plots of $\ln\ln [1/(1-f)]$ against (t) for $x = 1.5$.

due to a lower sintering rate of the sample containing Fe_2O_3 in excess of stoichiometry.

Fig. 6a shows the microstructure of the oxidized surface of the sample quenched from $900°$ C in air whose microstructure is shown in Fig. 5b. On the surface of the quenched sample some grey and white stripes are seen inside the grains. They are due to the oxidation of the surface during quench-

ing. These stripes inside the grains represent two different types of phase, i.e. $CuFe_2O_4$ and CuO.

Fig. 6b shows the microstructure of the above sample after prolonged heating in the oxygen atmosphere. This microstructure is different from the microstructure presented in Fig. 6a. CuO is present as globules at the grain boundaries of $CuFe_2O_4$ (in contrast with the lamellar pre-
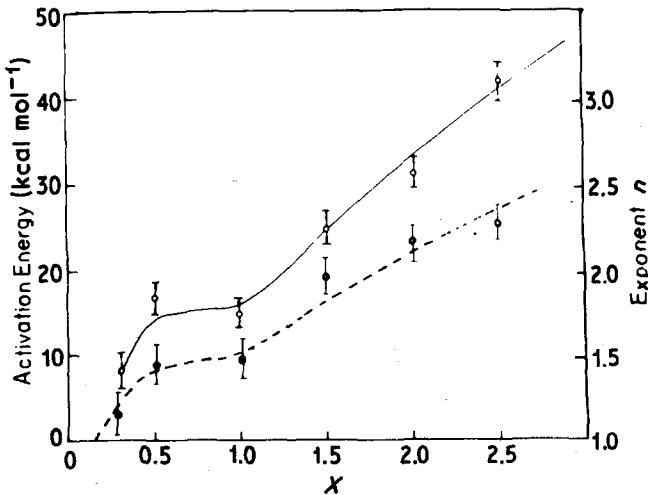

Figure 4 Plots of exponent n and activation energy against x.

TABLE III Rate constant at various temperatures

| Composition | k (sec^{-1}) | | | | |
	500° C	550° C	600° C	650° C	700° C
$CuFeO_2 + Cu_2O$	1.3×10^{-5}	1.67×10^{-5}	2.14×10^{-5}	3.36×10^{-5}	—
$CuFeO_2$	5.57×10^{-7}	—	2.0×10^{-6}	—	7.5×10^{-6}
$2CuFeO_2 + Fe_2O_3$	6.48×10^{-7}	—	—	3.23×10^{-7}	4.57×10^{-6}
$CuFeO_2 + Fe_2O_3$	3.39×10^{-9}	9.71×10^{-9}	2.5×10^{-8}	3.74×10^{-8}	—
$2CuFeO_2 + 3Fe_2O_3$	3.56×10^{-10}	1.189×10^{-9}	4.36×10^{-9}	6.84×10^{-9}	—
$CuFeO_2 + 2Fe_2O_3$	1.69×10^{-10}	9.736×10^{-10}	3.398×10^{-9}	1.186×10^{-9}	—

cipitation of Fig. 6a). When $x \geqslant 1$, CuO is not seen in the microstructures as shown in Fig. 7 b to e. Fig. 7b shows a single $CuFe_2O_4$ phase, which is stable up to 1050° C in an oxygen atmosphere.

Fig. 7 c to e shows two phases (one is grey and other is white). These are $CuFe_2O_4$ and Fe_2O_3 as per X-ray analysis. The concentration of white phase increases with x which confirms that the

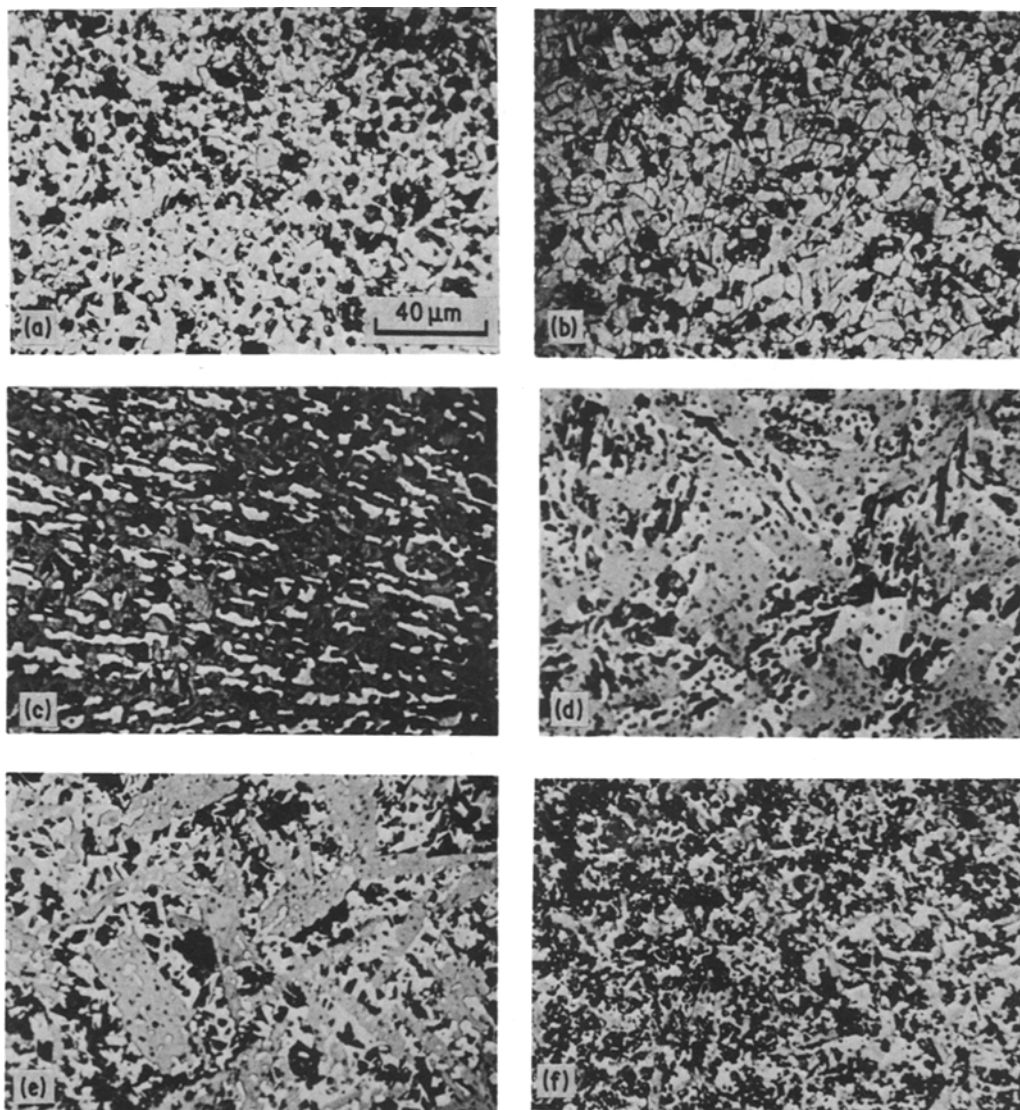Figure 5 Microstructures of different compositions $[CuO(Fe_2O_3)_x]$ in the Cu–Fe–O system sintered at 900° C in a nitrogen atmosphere and quenched (a) $x = 0.33$ (b) $x = 0.5$ (c) $x = 1.0$ (d) $x = 1.5$ (e) $x = 2.0$ and (f) $x = 2.5$.
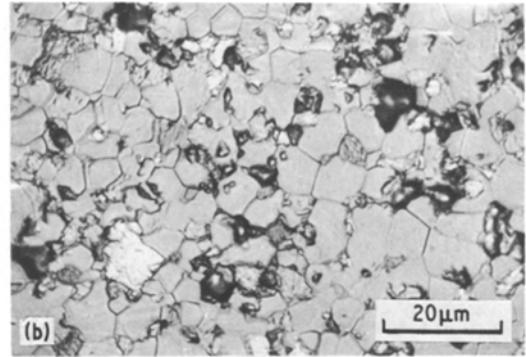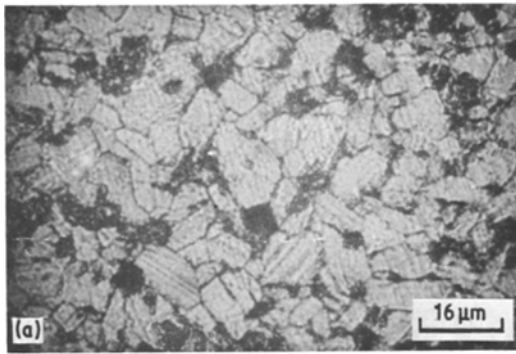
Figure 6 (a) Microstructure of the sample with composition 6 (Table I) after complete oxidation.
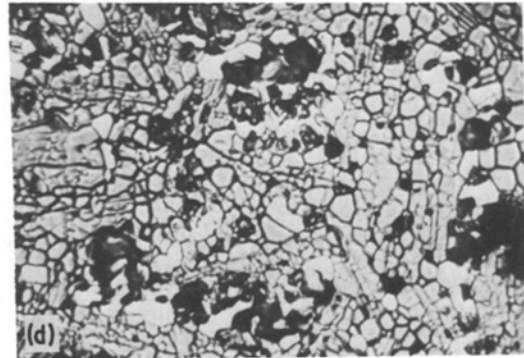

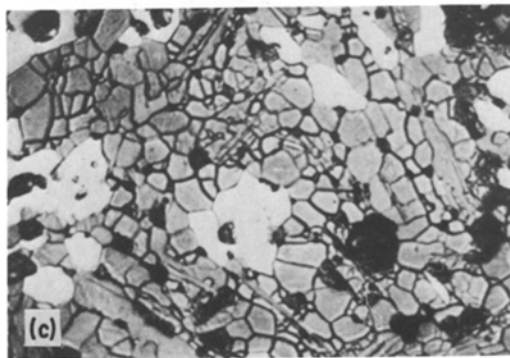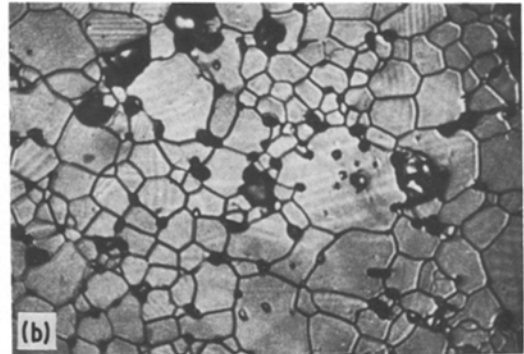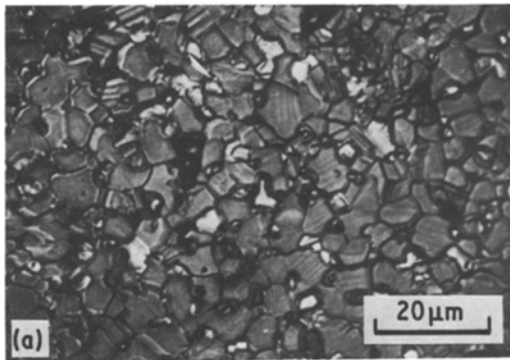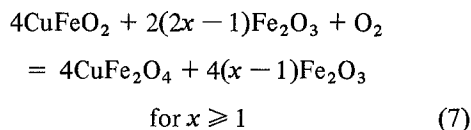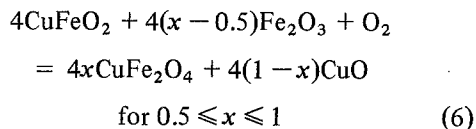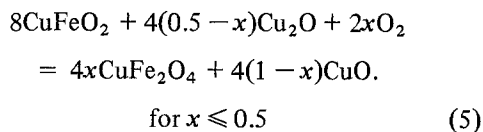*Figure 7* Microstructures of the oxidized samples of different compositions shown in Fig. 5 b to f (a) $x = 0.5$ (b) $x = 1.0$ (c) $x = 1.5$ (d) $x = 2.0$ and (e) $x = 2.5$.

grey phase is $CuFe_2O_4$ and the white phase is Fe_2O_3. In the Cu-rich sample shown in Fig. 7a, CuO precipitated along $CuFe_2O_4$ grains giving a microstructure similar to Fig. 6b. On comparing the microstructures of Fig. 7 b to e with Fig. 5 c to f, i.e. the volume fraction of $CuFe_2O_4$ seems to be more than that of $CuFeO_2$. Thus in the presence of oxygen in the atmosphere, inter-diffusion between $CuFeO_2$ and Fe_2O_3 took place and excess CuO or Fe_2O_3 precipitated.

4. Discussion

The results presented in Section 3 show that the samples of the Cu–Fe–O system in the reduced state have two phases i.e. $CuFeO_2$ and Cu_2O or Fe_2O_3 depending upon the composition. The oxidation of the sample ($CuFeO_2$) takes place when the equilibrium oxygen partial pressure $(p_{O_2}^{eq})$ of the composition is less than oxygen partial pressure (p_{O_2}) in the surrounding atmosphere, i.e. $p_{O_2} > p_{O_2}^{eq}$. Under the above conditions the sample adsorbs oxygen. The adsorbed oxygen acquires an electron from neighbouring Cu ions. Thus Cu ions become more positively charged and a metastable phase of "$Cu_2Fe_2O_5$" is formed. From this metastable phase the stable phases $CuFe_2O_4$ and CuO nucleate and grow in composition 3 of Table I. For a composition $x \geqslant 1$, Fe_2O_3 is present with $CuFeO_2$ and this Fe_2O_3 reacts with the oxidized metastable phase to give $CuFe_2O_4$, which is stable as shown in Fig. 8.

The oxidation of the samples at the surface may be explained by one or the other of the following equations.

$$8CuFeO_2 + 4(0.5-x)Cu_2O + 2xO_2$$
$$= 4xCuFe_2O_4 + 4(1-x)CuO.$$
$$\text{for } x \leqslant 0.5 \qquad (5)$$

$$4CuFeO_2 + 4(x-0.5)Fe_2O_3 + O_2$$
$$= 4xCuFe_2O_4 + 4(1-x)CuO$$
$$\text{for } 0.5 \leqslant x \leqslant 1 \qquad (6)$$

$$4CuFeO_2 + 2(2x-1)Fe_2O_3 + O_2$$
$$= 4CuFe_2O_4 + 4(x-1)Fe_2O_3$$
$$\text{for } x \geqslant 1 \qquad (7)$$

Equations 5, 6 and 7 show that for all compositions with $x < 1$, CuO precipitates out and for $x \geqslant 1$, a part of the second phase Fe_2O_3 which is already present dissolves. For further oxidation
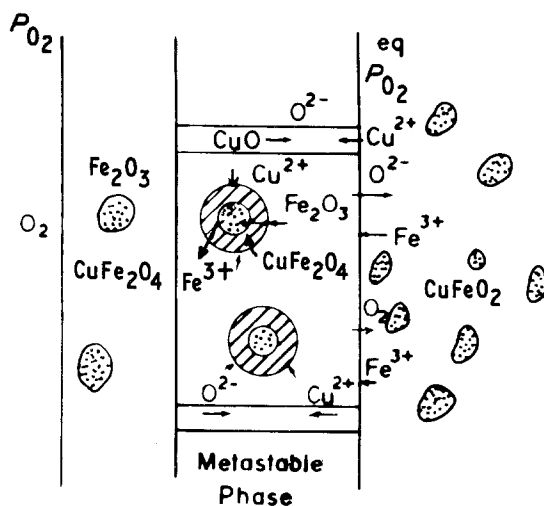

Figure 8 Schematic representation of the oxidation of $CuFeO_2$ with non-stoichiometric composition.

of the sample anions or cations should diffuse through the CuO, $CuFe_2O_4$ or Fe_2O_3 phases.

In the present work the activation energy for the oxidation of $CuFeO_2$ is the same for compositions 2 and 3 in Table I. The same values of activation energy for two different compositions indicates that in this composition range the mechanism of diffusion of ions during oxidation is the same. The results also indicate that in compositions 2 and 3 CuO precipitates in the oxidized layer. This together with the observation that the activation energy increases when CuO disappears as a second phase for $x > 1$, strongly suggests that diffusion of ions in the oxidized layer is predominantly through CuO when it is present. It is also well known that the activation energy for the diffusion of Cu ions through CuO is $18\,kcal\,mol^{-1}$ [11] whereas that for the diffusion of metal ions through a spinel lattice, range from 50 to $150\,kcal\,mol^{-1}$ [11].

The activation energy of oxidation increases significantly on increasing x above 1. The exponent n also increases in this region indicating a possible change in mechanism of oxidation. Beyond the composition with x equal to 1, no CuO phase is stable in the oxidized region and the increase in n from 1.3 to 2.3 indicates that the oxidation process becomes a two dimensional one. This is expected since in this composition range, as discussed earlier, oxidation proceeds by formation of an oxygen rich metastable phase, which converts to $CuFe_2O_4$ by interdiffusion of ions as shown in Fig. 8.

The interdiffusion process of Cu^{2+} and Fe^{3+} ions between Fe_2O_3 and metastable $(Cu_2Fe_2O_5)$ phases seems to be similar to the interdiffusion of metal ions between metallic oxide systems like $MgO-Al_2O_3$, $MgO-Fe_2O_3$ etc. [11]. The activation energy for the diffusion process of oxygen or metal ions in Fe_2O_3 and spinel ferrites varies from 50 to $150\,kcal\,mol^{-1}$ [11]. In the $Cu-Fe-O$ system not only the interdiffusion of Ce/Fe ions between the Fe_2O_3 and the metastable phase is taking place but also the nucleation of CuO, which is also a prominent factor.

The activation energy for the diffusion of the $Cu-Fe-O$ system is found to decrease on decreasing x below 0.5. Samples with these compositions have two phases i.e. $CuFeO_2$ and Cu_2O in the reduced state. For these, adsorption of oxygen ions and the recombination of the diffusing ions become the rate controlling factors. For adsorption and recombination the activation energy is very low [12]. Therefore, it can be concluded that on increasing the concentration of Cu_2O the adsorption and recombination processes start to dominate, resulting in a lower activation energy.

A model proposed for explaining the oxidation of powdered material of stoichiometric composition agrees quite well with the microstructure shown in Fig. 6a. The grey and white lines inside the grains represent two products of the oxidation of $CuFeO_2$. These are $CuFe_2O_4$ and CuO, according to the reaction

$$4CuFeO_2 + O_2 \leftrightharpoons 2CuFe_2O_4 + 2CuO$$
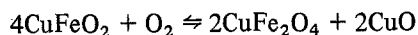
because in an oxygen atmosphere only $CuFe_2O_4$, CuO and Fe_2O_3 are stable. Prolonged heating of $CuFeO_2$ in an oxygen atmosphere causes CuO to spheroidize and such spheroids of CuO are found at the grain boundaries of $CuFe_2O_4$. In the non-stoichiometric compositions, interdiffusion between $CuFeO_2$ and Fe_2O_3 starts to form $CuFe_2O_4$ at the interfaces. This reaction continues until the $CuFeO_2$ phase completely disappears. This is a slow process, therefore, on prolonged oxidation grains of $CuFe_2O_4$ also begin to grow. Excess Fe_2O_3, greater than the stoichiometric composition of $CuFe_2O_4$, remains unreacted at some places.

References
1. G. C. JAIN, B. K. DAS and R. AVTAR, *J. Mater. Sci.* 12 (1977) 1903.
2. J. THERY and R. COLLONGUES, *Compt. Rend.* 254 (1962) 685.
3. H. J. LEVINSTEIN, F. J. SCHNEHLER and E. M. G. YORGY, *J. Appl. Phys.* 36 (1965) 1163.
4. Z. SIMSA, *IEEE Trans. Mag.* 5 (1969) 592.
5. T. TAMAGNCHI and T. SHIRASHI, *J. Amer. Ceram. Soc.* 52 (1969) 401.
6. G. C. JAIN, B. K. DAS and R. AVTAR, *Indian J. Pure Appl. Phys.* 8 14 (1976) 796.
7. *Idem*, unpublished work, 1977.
8. M. AVRAMI, *J. Chem. Phys.* 7 (1939) 1103.
9. J. W. CHRISTIAN, "The Theory of transformation in Metals and Alloys", part 4 (Pergamon Press, New York, 1974) p. 19.
10. A. M. M. GADALLA and J. WHITE, *Trans. Brit. Ceram. Soc.* 65 (1966) 4.
11. B. I. VOLTAKS, "Diffusion in Semiconductors", (Inforserach Limited, London, 1963), p. 281.
12. E. R. S. WINTER, *J. Chem. Soc.* (1955) 3824.